Mechanism of Ion Permeation in Skeletal Muscle Chloride Channels

Christoph Fahlke,*‡ Christine Dürr,*‡ and Alfred L. George, Jr.*‡

From the *Department of Medicine, and ‡Department of Pharmacology, Vanderbilt University School of Medicine, Nashville, Tennessee 37232-2372

ABSTRACT Voltage-gated Cl^- channels belonging to the ClC family exhibit unique properties of ion permeation and gating. We functionally probed the conduction pathway of a recombinant human skeletal muscle Cl^- channel (hClC-1) expressed both in *Xenopus* oocytes and in a mammalian cell line by investigating block by extracellular or intracellular I^- and related anions. Extracellular and intracellular I^- exert blocking actions on hClC-1 currents that are both concentration and voltage dependent. Similar actions were observed for a variety of other halide (Br^-) and polyatomic (SCN^-, NO_3^-, $CH_3SO_3^-$) anions. In addition, I^- block is accompanied by gating alterations that differ depending on which side of the membrane the blocker is applied. External I^- causes a shift in the voltage-dependent probability that channels exist in three definable kinetic states (fast deactivating, slow deactivating, nondeactivating), while internal I^- slows deactivation. These different effects on gating properties can be used to distinguish two functional ion binding sites within the hClC-1 pore. We determined K_D values for I^- block in three distinct kinetic states and found that binding of I^- to hClC-1 is modulated by the gating state of the channel. Furthermore, estimates of electrical distance for I^- binding suggest that conformational changes affecting the two ion binding sites occur during gating transitions. These results have implications for understanding mechanisms of ion selectivity in hClC-1, and for defining the intimate relationship between gating and permeation in ClC channels.

KEY WORDS: chloride channel • skeletal muscle • permeation • electrophysiology

INTRODUCTION

The molecular cloning of a voltage-gated Cl^- channel from the electric organ of *Torpedo* (Jentsch et al., 1990) and the subsequent characterization of a large number of mammalian homologs (Jentsch, 1994) has established a new gene family (ClC-family) lacking any structural similarity to other known ion channels. At present, the basic mechanisms responsible for ion permeation and gating in ClC channels are incompletely understood.

We have focused on the human muscle ClC-isoform, hClC-1. This dimeric channel (Fahlke et al., 1997*b*) is important physiologically for the control of sarcolemmal excitability and it is the genetic locus in mouse, man, and goat for a specific form of inherited myotonia (Steinmeyer et al., 1991; Koch et al., 1992; George et al., 1993; Beck et al., 1996). We have previously characterized a recombinant human ClC-1 (hClC-1) expressed heterologously in both *Xenopus* oocytes and human embryonic kidney cells (Fahlke et al., 1995, 1996), and found that its functional attributes are identical to native skeletal muscle channels (Fahlke and Rüdel, 1995).

Address correspondence to Dr. Christoph Fahlke, Department of Medicine and Pharmacology, Vanderbilt University Medical Center, 21st Avenue South at Garland, Nashville, TN 37232-2372. Fax: 615-343-7156; E-mail: cfahlke@mbio.mc.vanderbilt.edu

Investigation of the dependence of gating properties on pH and chloride concentrations has helped us to develop a first gating model of this channel (Fahlke et al., 1996). Gating of hClC-1 appears to be mediated by two structurally distinct mechanisms: a fast voltage-dependent process and a slow voltage-independent process controlling opening and closing transitions through block of the pore by a probable cytoplasmic gate (Fahlke et al., 1996). The voltage-dependent process governs the distribution of open channels in three kinetically distinct states: fast deactivating, slow deactivating, and nondeactivating. More recently, we have characterized an hClC-1 mutation (G230E) that causes autosomal dominant myotonia congenita and confers altered ion selectivity on the channel (Fahlke et al., 1997*a*). In that report, examination of the effect of I^- on both wild-type and mutant channels provided preliminary evidence for the existence of two distinct anion binding sites within the hClC-1 pore.

To improve our understanding of the basic properties of the hClC-1 pore, and to learn more about the relationships between gating and permeation, we now investigate in more detail the interaction of I^- and other analogs of the normal permeant ion with these binding sites. One specific goal of this investigation was to determine if the different conducting states defined by our gating model exhibit differences in ion binding characteristics. This work reveals clear differences in the characteristics of I^- block exhibited by the three ki-

netic states and implies that conformational changes within the conduction pathway are occurring during gating. We also define the hClC-1 conduction pathway as a multi-ion pore, and argue in favor of an ion-selectivity mechanism based on differential ion binding. These results provide much needed characterization of the ion permeation process and clarify a functional link between gating and ion conductance in hClC-1.

METHODS

Oocyte Preparation and Two-Electrode Voltage Clamp

Isolation, maintenance, and cRNA injection of *Xenopus* oocytes were performed as previously described (Beck et al., 1996). Standard two-microelectrode voltage clamp was performed using an amplifier (OC-725B; Warner Instruments Corp., Hamden, CT). Microelectrodes were pulled from borosilicate glass to have a resistance between 0.7 and 1.3 MΩ when filled with 3 M KCl. The oocytes were bathed in ND-96 solution (Dascal et al., 1986) containing 96 mM NaCl, 4 mM KCl, 1.8 mM $CaCl_2$, 1 mM $MgCl_2$, 5 HEPES (adjusted to pH 7.4 with NaOH). To test the effect of various anions on hClC-1 currents, the bathing solution was changed to a modified ND-96 in which NaCl was replaced by an equimolar quantity of NaSCN, $NaNO_3$, $NaCH_3SO_3$, Na-cyclamate, or Na-gluconate. For the calculation of relative current amplitudes, both instantaneous and late current amplitudes were divided by the instantaneous current amplitude measured at −145 mV in the same cell using standard ND-96 solution. In general, endogenous oocyte chloride currents can be distinguished easily from hClC-1 currents by their different kinetics. Among the various reported types of endogenous oocyte chloride currents, calcium-activated chloride currents bear the closest resemblance to hClC-1. However, calcium-activated chloride currents display a clear activating phase upon voltage steps to positive potentials (Tokimasa and North, 1996) that is absent in hClC-1-expressing cells at similar test potentials (Fahlke et al., 1996). Therefore, oocytes exhibiting an activating component larger than 1 μA at +55 mV were excluded from analysis.

Whole-Cell Recording

HEK-293 cells (CRL 1573; American Type Culture Collection, Rockville, MD) were stably transfected by the calcium phosphate precipitation method using the plasmid pRc/CMV-hClC-1 as described (Fahlke et al., 1995).

Standard whole-cell recording (Hamill et al., 1981) was performed using an Axopatch 200A amplifier (Axon Instruments, Foster City, CA). Pipettes were pulled from borosilicate glass and had resistances of 0.6–1.0 MΩ. Cells with peak current amplitudes <10 nA were used for analysis. More than 60% of the series resistance was compensated by an analog procedure. The calculated voltage error due to series resistance was always <5 mV. No digital leakage or capacitive current subtraction was used. Currents were low pass filtered with an internal amplifier filter and digitized with sampling rates at least three times larger than the filtering frequency using pClamp (Axon Instruments). Cells were held at 0 mV for at least 15 s between test pulses.

The standard bath solution contained (mM): 140 NaCl, 4 KCl, 2 $CaCl_2$, 1 $MgCl_2$, and HEPES, pH 7.4. In experiments testing the effect of external I^- or other anions, the standard bath solution was modified by replacing variable amounts of NaCl with equimolar quantities of NaI or the corresponding sodium salt of other anions. For determination of I^- dissociation constants (K_D) for the extracellular ion binding site, measurements were initially made in an extracellular solution composed of (mM): 140 Na-gluconate, 4 KCl, 2 $CaCl_2$, 1 $MgCl_2$, 5 HEPES, pH 7.4, and then changed to a modified solution in which Na-gluconate was replaced by NaI. For experiments with I^--containing solutions, agar bridges (3 M KCl in 0.1% agar) were used to connect the bath solution to the amplifier.

The standard pipette solution was (mM): 130 NaCl, 2 $MgCl_2$, 5 EGTA, 10 HEPES, pH 7.4. In some experiments, CsCl was substituted for NaCl without appreciable differences in the results. For determination of K_D for I^- binding to the intracellular site, measurements were made in a pipette solution containing (mM): 50 NaCl, 80 Na-gluconate, 2 $MgCl_2$, 5 EGTA, 10 HEPES, pH 7.4, or in solutions in which Na-gluconate was replaced by equimolar NaI. All solutions were adjusted to pH 7.4 with NaOH or CsOH. Unless otherwise stated, standard solutions were used. For experiments with I^--containing solutions, agar bridges (3 M KCl in 0.1% agar) placed inside the patch pipette were used to connect solutions with the amplifier.

The concentration dependence of the reversal potential was determined in stably transfected HEK 293 cells under bi-anionic conditions using three different intracellular solutions (mM): (*a*) 44 NaI, 5 EGTA, 10 HEPES, 200 sucrose; (*b*) 88 NaI, 5 EGTA, 10 HEPES, 100 sucrose; (*c*) 132 NaI, 5 EGTA, 10 HEPES, in combination with three different extracellular solutions (mM): (*a*) 49 NaCl, 1 $CaCl_2$, 5 HEPES, 200 sucrose; (*b*) 98 NaCl, 1 $CaCl_2$, 5 HEPES, 100 sucrose; (*c*) 147 NaCl, 1 $CaCl_2$, 5 HEPES. All solutions were adjusted to pH 7.4 with NaOH. Reversal potentials were measured after a 2–3 min equilibration time period after establishment of the whole-cell configuration.

Excised Patch Recording

For recording from inside-out excised patches (see Fig. 7), pipettes were pulled from borosilicate glass to have resistances between 1.2 and 2.0 MΩ, coated with Sylgard, and filled with standard extracellular solution. The bath solution was identical to the standard intracellular solution described above for whole-cell recording. Using a solution changing system (SF-77 Perfusion Fast-Step System; Warner Instrument Corp.), the intracellular membrane side of the patch was first exposed to a solution containing (mM): 50 NaCl, 80 Na-gluconate, 2 $MgCl_2$, 5 EGTA, 10 HEPES, pH 7.4, and baseline recordings were made. Subsequently, the solution was changed to (mM): 50 NaCl, 50 NaI, 30 Na-gluconate, 2 $MgCl_2$, 5 EGTA, 10 HEPES, pH 7.4, and the measurements were repeated.

Data Analysis

Current deactivation was tested after a 50-ms prepulse to +55 mV. The time course of current deactivation was fit with an equation containing a sum of two exponentials and a time-independent value as follows: $I(t) = a_1\exp(-t/\tau_1) + a_2\exp(-t/\tau_2) + d$, where a_1, a_2, and d are amplitude terms, τ_1 and τ_2 are time constants for fast and slow deactivation, respectively. The fractional current amplitudes were calculated by dividing by the peak current amplitude (I_{max}) as follows: $A_1 = a_1/I_{max}$, $A_2 = a_2/I_{max}$, $C = d/I_{max}$ (Fahlke et al., 1996).

For the calculation of I^- dissociation constants (K_D) for the external binding site, fractional current amplitudes (A_1, A_2, and C) determined at several test potentials were plotted versus the extracellular $[I^-]$. The K_D values at given test potentials were obtained as described in RESULTS. Calculation of K_D for the intracellular binding site was performed by plotting reciprocal values of

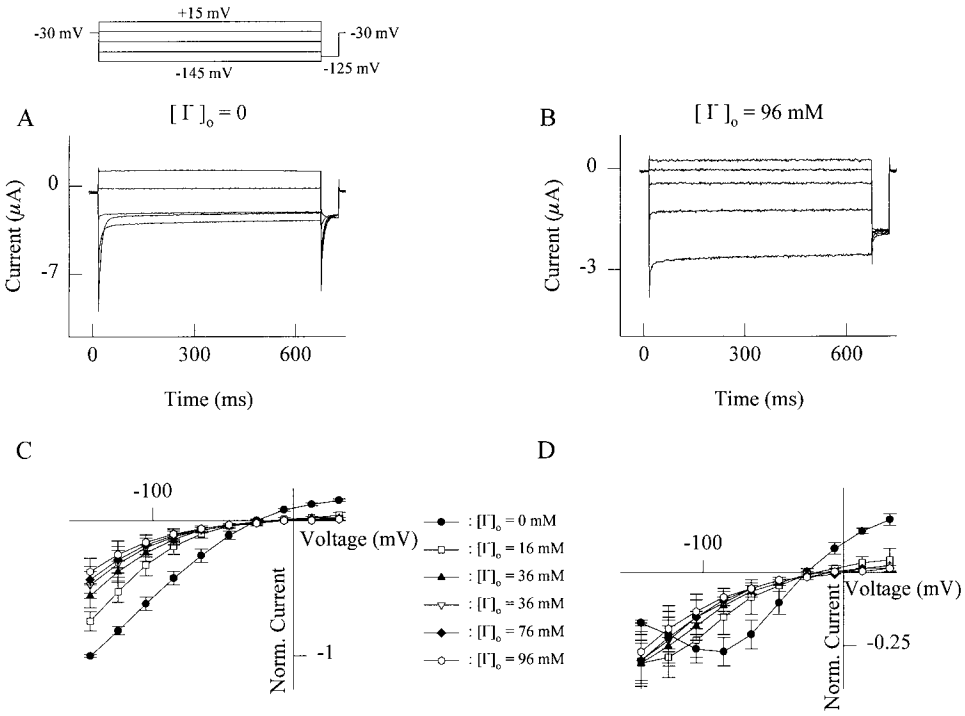

FIGURE 1. Effect of extracellular I^- on hClC-1 expressed in *Xenopus* oocytes. (*A*) Current responses to voltage steps from a holding potential of −30 mV in 40-mV steps from −145 to +15 mV measured in standard extracellular solution. Each test pulse is followed by a step to −125 mV. (*B*) Current responses to the same pulse protocol in the same oocyte as in *A* after substitution of 96 mM NaCl by an equimolar concentration of NaI. (*C*) Voltage dependence of the instantaneous current amplitude for different extracellular [I^-]. Data represent mean ± SEM from four different cells (every cell was tested with each [I^-]). Current amplitudes were normalized to the instantaneous current amplitude measured at −145 mV in the absence of extracellular I^-. (*D*) Voltage dependence of the late current amplitude obtained from the same data set shown in *C*. Data were normalized in the same way as in *C*.

the deactivation time constants (τ_1^{-1}, τ_2^{-1}) versus the intracellular [I^-], and then deriving K_D as a fit parameter by the method explained in RESULTS.

RESULTS

Block of hClC-1 by External I^-

To examine the effect of external I^- on hClC-1, initial experiments were performed in *Xenopus* oocytes to permit current recording from the same cell in the presence of various external solutions. Fig. 1 illustrates current recordings made in oocytes expressing hClC-1 before (Fig. 1 *A*) and after (Fig. 1 *B*) substitution of 96 mM NaCl by equimolar NaI in the extracellular solution. External I^- causes a significant reduction in the 'instantaneous' current amplitude measured 2 ms after hyperpolarizing voltage steps from a holding potential of −30 mV, and shifts the reversal potential to a more positive voltage (Fig. 1, *C* and *D*), indicating a greater permeability of hClC-1 for Cl^- than I^-. In addition, external I^- affects hClC-1 gating, resulting in less complete deactivation (Fig. 1 *B*) and loss of the characteristic inverted bell shape of the steady state current–voltage relationship observed at negative test potentials (Fig. 1 *D*). Similar effects of external I^- on hClC-1 have been observed in mammalian cells by whole cell recording (Fahlke et al., 1997*a*).

The effect of external I^- on hClC-1 current amplitude is concentration and voltage dependent. Increasing the external I^- from 16 to 96 mM causes a concentration-dependent reduction of instantaneous (Fig. 1 *C*) normalized inward current amplitudes recorded at voltages negative to the reversal potential. At voltages positive to the reversal potential, reduction of normalized instantaneous outward current amplitude is near saturation at 16 mM I^-. Thus, external I^- reduces both inward and outward current, having its greatest effect on outward currents measured at positive potentials. These data are consistent with voltage-dependent block of hClC-1 by external I^-.

Block of hClC-1 by Other Extracellular Anions

We investigated the effect of other extracellular anions on hClC-1 expressed in oocytes by substituting 48 mM Cl^- in the external solution by equimolar amounts of Br^-, SCN^-, NO_3^-, $CH_3SO_3^-$, cyclamate, or gluconate. Fig. 2 shows representative voltage-clamp recordings for control conditions (Fig. 2 *A*), 48 mM $CH_3SO_3^-$ (Fig. 2 *B*), 48 mM NO_3^- (Fig. 2 *C*), and 48 mM SCN^- (Fig. 2 *D*). The equimolar substitution of Cl^- with each of these anions causes a variable reduction of inward current amplitudes within the negative potential range. These effects vary depending on the replaced anion

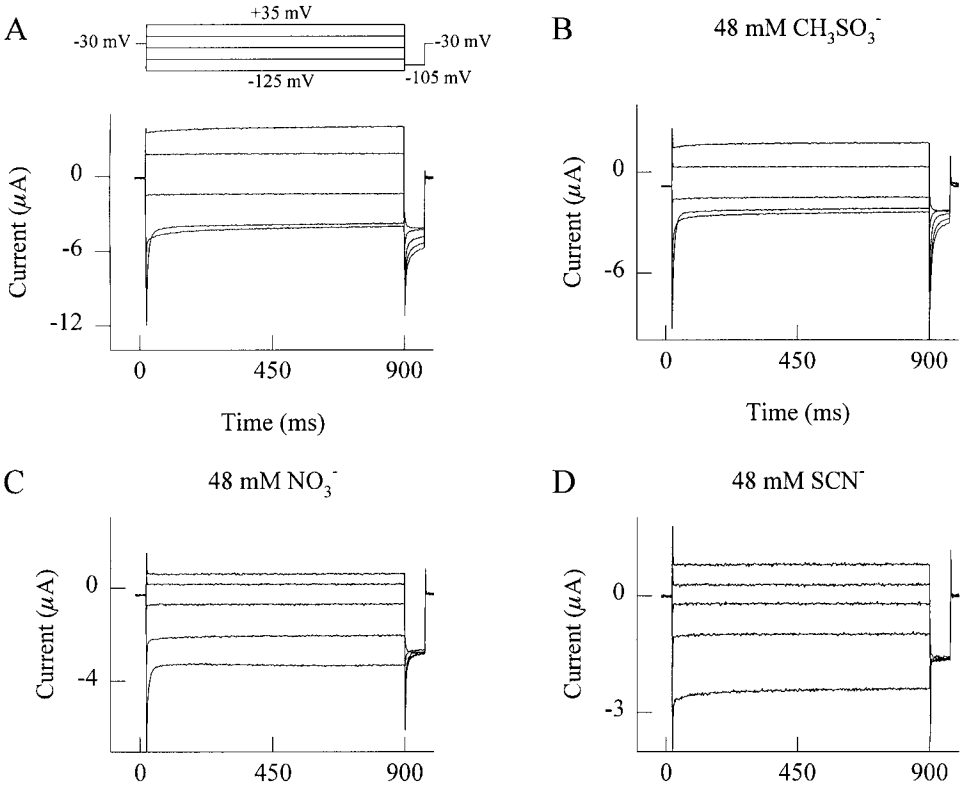

FIGURE 2. Effect of other extracellular anions on hClC-1 expressed in *Xenopus* oocytes. Current responses to voltage steps between −125 and +35 mV in 40-mV steps from a holding potential of −30 mV from a single oocyte are shown. In *A*, the extracellular solution was ND-96. For the three other recordings, 48 mM NaCl was substituted by an equimolar concentration of $NaCH_3SO_3$ (*B*), $NaNO_3$ (*C*), and NaSCN (*D*).

and therefore are not simply caused by reduction of the external Cl^- concentration.

Plots of normalized current amplitudes versus voltage for seven different ionic conditions are shown in Fig. 3. Fig. 3, *A* and *B* shows substitution experiments with anions believed to be permeant (Br^-, SCN^-, NO_3^-), while Fig. 3, *C* and *D* illustrate data from experiments in which the substituted anions were suspected of being impermeant ($CH_3SO_3^-$, cyclamate, and gluconate). All anion substitutions cause a shift of the reversal potential to more positive voltages, indicating lower permeability, relative to Cl^-, for each of the tested anions. In addition, normalized inward and outward current amplitudes are blocked by all anions except gluconate (the effect of gluconate on outward current can be explained by the reduction of external Cl^- concentration). Blocking anions also affect gating properties, as can be observed in the steady state current–voltage plots, especially at voltages negative to the reversal potential (Fig. 3, *B* and *D*). The blocking potency and the potency to change current kinetics are correlated (Fig. 3 *E*).

Gating Effects of External I^- on hClC-1

We next studied in more detail the effect of external I^- on hClC-1 gating properties by using whole-cell recording of HEK-293 cells stably expressing the channel (Fahlke et al., 1996). Either in the absence or presence of extracellular I^-, the time course of current deactivation upon hyperpolarizing voltage steps can be fit with a sum of two exponentials and a constant value. These fits provide two different data sets: the time constants of deactivation (τ_1 and τ_2 for fast and slow deactivation, respectively), and the fractional amplitudes of two deactivating and one nondeactivating current components. We interpret the fractional current amplitudes as estimates of the proportion of channels existing in each of three different kinetic states: fast, slow, and nondeactivating (Fahlke et al., 1996).

Fig. 4 illustrates the effect of external I^- on these gating parameters for hClC-1 stably expressed in HEK-293 cells. Replacement of 40 mM NaCl by an equimolar concentration of NaI in the external solution has no effect on the time constants of deactivation (Fig. 4 *A*), but there are dramatic changes in the voltage dependence of the fractional current amplitudes. In Fig. 4, *B–D*, a pronounced concentration-dependent leftward shift of the fractional amplitudes for fast deactivating (Fig. 4 *B*, A_1), slow deactivating (Fig. 4 *C*, A_2), and nondeactivating (Fig. 4 *D*, *C*) current components can be seen. In the negative voltage range in which this effect was observed, there is an increase of the fraction of channels that either deactivate with a slow time constant or do not deactivate at all. This behavior of the fractional current amplitudes explains the less com-

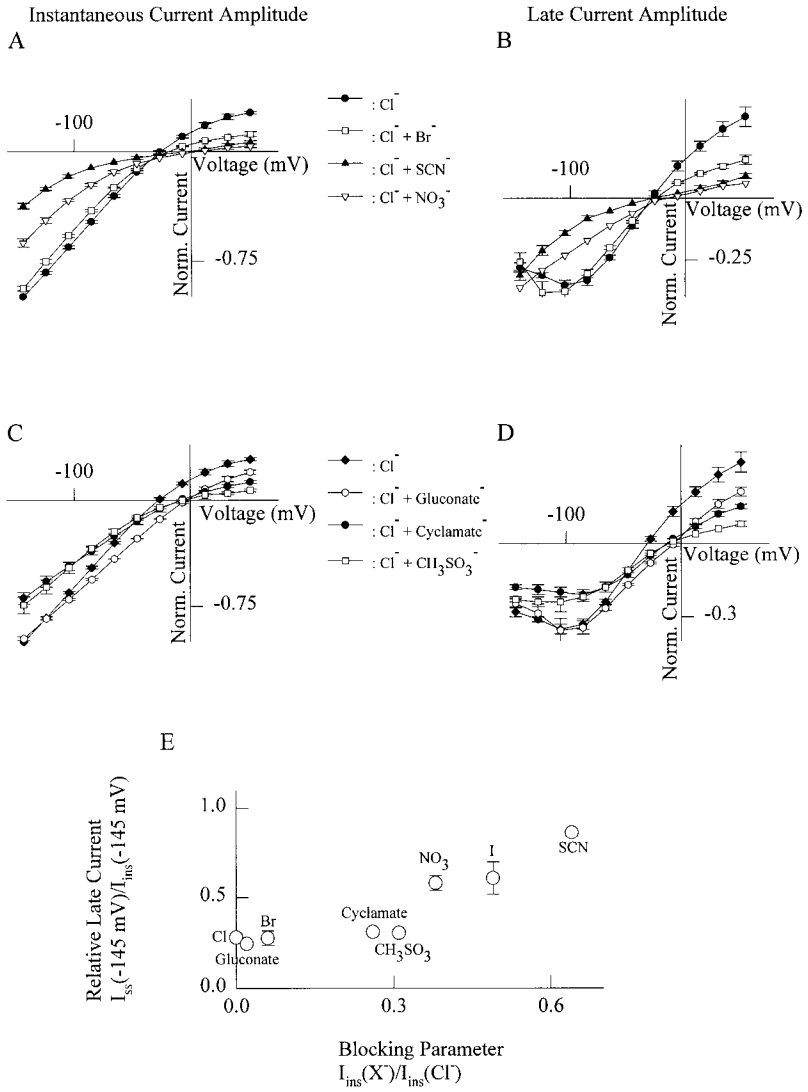

FIGURE 3. Normalized current–voltage relationships for hClC-1 in various extracellular solutions. For each anion tested, 48 mM NaCl was replaced by equimolar NaX, with X denoting different anions. For each anion, instantaneous (*A* and *C*) and steady state (*B* and *D*) currents were measured during voltage steps from a holding potential of −30 mV and normalized to the instantaneous current amplitude at −145 mV for the same oocyte in ND-96. Each point represents mean ± SEM for at least three cells. (*A*) Voltage dependence of the instantaneous current amplitude for extracellular solutions containing 96 mM NaCl (●), 48 mM NaCl + 48 mM NaBr (□), 48 mM NaCl + 48 mM NaSCN (▲), and 48 mM NaCl + 48 mM $NaNO_3$ (▽). (*B*) Voltage dependence of the steady state amplitudes from the same recordings as shown in *A*. (*C*) Voltage dependence of the instantaneous current amplitude for extracellular solutions containing 96 mM NaCl (◆), 48 mM NaCl + 48 mM Na-gluconate (○), 48 mM NaCl + 48 mM Na-cyclamate (●), and 48 mM NaCl + 48 mM $NaCH_3SO_3$ (□). (*D*) Corresponding steady state values from the experiment shown in *C*. (*E*) Correlation between a blocking parameter (I_{peak} in the presence of 48 mM anion divided by I_{peak} in the presence of Cl^- measured at −145 mV) and relative late current (I_{late} divided by I_{peak} measured at −145 mV) for various extracellular anions.

plete deactivation observed in the presence of external I^- (Fig. 1 *B*).

Kinetic States Differ in Affinity for External I^-

Because hClC-1 is conducting in all three kinetic states (Fahlke et al., 1996) and I^- binds to a site within the conduction pathway (Fahlke et al., 1997*a*), it is reasonable to hypothesize that I^- can bind to the channel whether it is in the fast, slow, or nondeactivating state (SCHEME 1).

$$\begin{array}{ccccc} A_1 & \rightleftharpoons & A_2 & \rightleftharpoons & C \\ k_{off,1} \downarrow\uparrow k_{on,1} & & k_{off,2} \downarrow\uparrow k_{on,1} & & k_{off,c} \downarrow\uparrow k_{on,c} \\ A_1\text{-}I^- & \rightleftharpoons & A_2\text{-}I^- & \rightleftharpoons & C\text{-}I^- \end{array}$$

(SCHEME 1)

In this scheme, the channel can exist in one of three states, A_1 (fast deactivating), A_2 (slow deactivating), and C (nondeactivating) in the absence of I^-, and similarly it can exist in one of three states (A_1-I^-, A_2-I^-, and C-I^-) when I^- is bound. The I^- concentration dependence of the fractional current amplitudes (Fig. 4 *A*) indicates that the rate constants connecting the I^--bound states (A_1-I^-, A_2-I^-, and C-I^-) are different from those connecting the unbound states (A_1, A_2, C). At saturating I^- concentration, all channels are occupied by I^-, and the measured fractional current amplitudes thus represent the distribution of channels only in the three I^--bound kinetic states. At all voltages, the measured fractional amplitudes of the fast (A_1) and the slow (A_2) deactivating component reach limiting values of zero (Fig. 5, *A* and *B*) at high I^- concentrations. Correspondingly, the constant fractional amplitude (C) approaches a value of one (Fig. 5 *C*). Therefore, reaction rate constants between the three different I^- bound states (A_1-I^-, A_2-I^-,

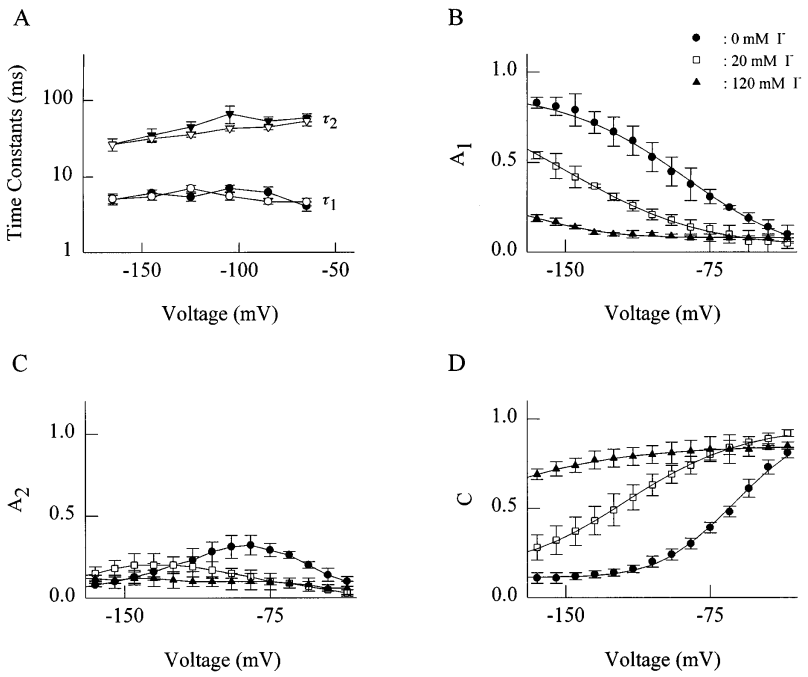

FIGURE 4. Effect of extracellular I^- on hClC-1 deactivation. (*A*) Voltage dependence of fast and slow time constants in the absence (*filled symbols*) or presence (*open symbols*) of 40 mM I^-. (*B–D*) Voltage dependence of the fractional amplitudes A_1 (*B*), A_2 (*C*), and C (*D*) determined in the presence of three different extracellular I^- concentrations. Extracellular [I^-] was increased by replacing NaCl with equimolar amounts of NaI in the external solution. Each point represents mean ± SEM for at least three cells.

and C-I^-) must be negligible, and we can simplify the state diagram (SCHEME II).

$$\begin{array}{ccccc} A_1 & \rightleftharpoons & A_2 & \rightleftharpoons & C \\ k_{off,1} \updownarrow k_{on,1} & & k_{off,2} \updownarrow k_{on,1} & & k_{off,c} \updownarrow k_{on,c} \\ A_1\text{-}I^- & & A_2\text{-}I^- & & C\text{-}I^- \end{array}$$

(SCHEME II)

In this scheme, each I^- bound state can be reached only from the corresponding unbound state. Transitions between corresponding bound and unbound states can be characterized by two rate constants: a first order dissociation constant (k_{off}) and a second order association constant (k_{on}) for I^-. The proportion of channels in a particular kinetic state (i) occupied by I^- is given by $[I^-]/([I^-] + K_{D,i})$, where $K_{D,i}$ is a dissociation constant equal to the ratio $k_{off,i}/k_{on,i}$. This expression assumes that binding of I^- to the channel equilibrates much faster than the voltage-dependent gating process, and that only one external I^- binds to the channel in each kinetic state. The latter assumption is tested below. The experimentally determined fractional current amplitude for a given kinetic state (A_i) in the presence of I^- is a weighted mixture of two different probabilities: $p_I(i)$ for I^- occupied channels, and $p_o(i)$ for unoccupied channels; these variables are related in the following equation:

$$A(i) = \frac{[I^-]}{[I^-] + K_{D,i}} p_I(i) + \left(1 - \frac{[I^-]}{[I^-] + K_{D,i}}\right) p_o(i) \quad (1)$$

which simplifies to:

$$A(i) = p_o(i) + \frac{[I^-]}{[I^-] + K_{D,i}} (p_I(i) - p_o(i)) \quad (2)$$

in which i is a given kinetic state (fast, slow, or nondeactivating), $A(i)$ is the probability for a given state at a specific I^- concentration and test voltage, while p_o denotes the probability without and p_I with I^- bound to the channel. This probability expression can provide information on the dissociation constant for I^- in the three different kinetic states, and by analyzing data from several test potentials, we can determine the voltage dependence of K_D.

This analysis does not exclude the possibility that more than one external binding site exerting similar effects on gating exist per channel pore. To test this possibility, we determined Hill coefficients (n) from plots of fractional current amplitude versus [I^-] by fitting a modified version of Eq. 2:

$$A(i) = p_o(i) + \frac{[I^-]^n}{[I^-]^n + K_{D,i}^n} (p_I(i) - p_o(i)) \quad (3)$$

We determined the concentration dependence of the effect of external I^- on the three fractional current amplitudes (Fig. 5). Fractional current amplitudes were determined from current recordings made during various test pulses between −75 and −165 mV after a max-

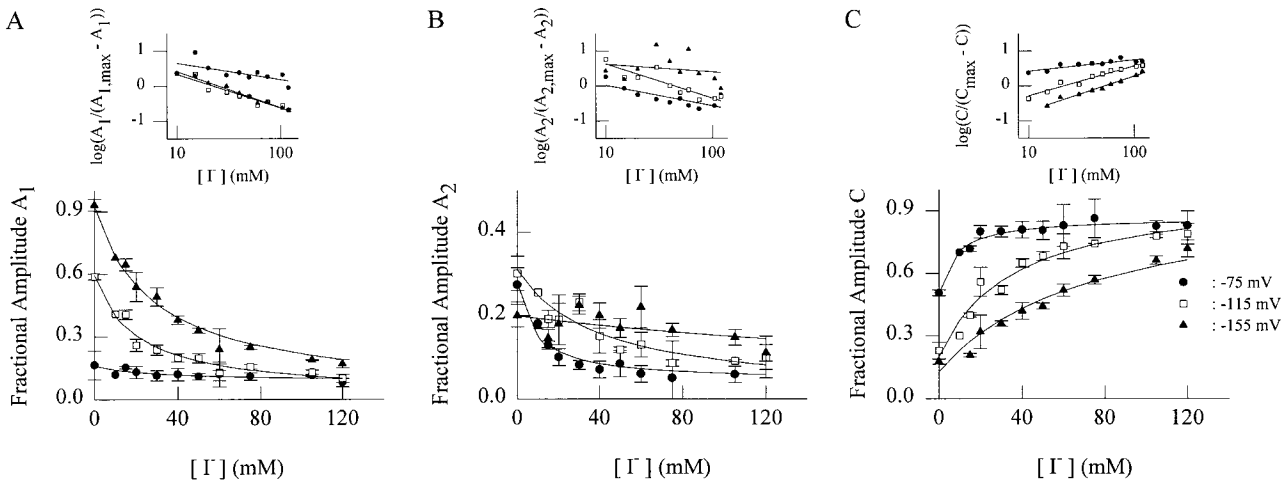

FIGURE 5. Relationship between extracellular I^- concentration and fractional current amplitudes. Fractional current amplitudes were determined at three different test potentials (−75, −115, and −165 mV) as described in METHODS. Solid lines represent fitted hyperbola (see text) to the measured data. Each point represents mean ± SEM for at least three cells. (*A*) Fast deactivating fractional current amplitude, A_1. (*B*) Slow deactivating fractional current amplitude, A_2. (*C*) Nondeactivating fractional current amplitude, C. Insets show transformations of the data with fitted regression lines as described in RESULTS. Hill coefficients determined from the regression lines are as follows: A_1: 0.47, 0.96, and 1.00; A_2: 0.59, 0.98, and 0.22; C: 0.31, 0.86, and 0.99 for test potentials of −75, −115, and −155 mV, respectively.

imally activating prepulse (+55 mV) in the presence of different I^- concentrations. To avoid effects caused by changing concentrations of Cl^-, the extracellular Cl^- concentration was held constant (10 mM) and bath gluconate was varied inversely with changes in I^- concentration. Gluconate has no effect on gating properties of hClC-1 (Fig. 3).

We evaluated our model in two steps. First, we determined the Hill coefficient for each fractional current amplitude by fitting regression lines of the log ($A/(A_{max} - A)$) vs. log([I^-]) relationship where A represents the different fractional amplitudes (Fig. 5, *A–C*, *insets*). All calculated slopes had values ≤1, consistent with a single external I^- binding site. Next, we fitted Eq. 2 to the data (Fig. 5, *A–C*) to obtain the voltage dependence of the dissociation constants for I^- in each kinetic state and the voltage dependence of p_o and p_I (these fit parameters are plotted in Fig. 6, see below). For the A_1, A_2, and C components, the data are well fit with a single hyperbola, although data for the slow de-

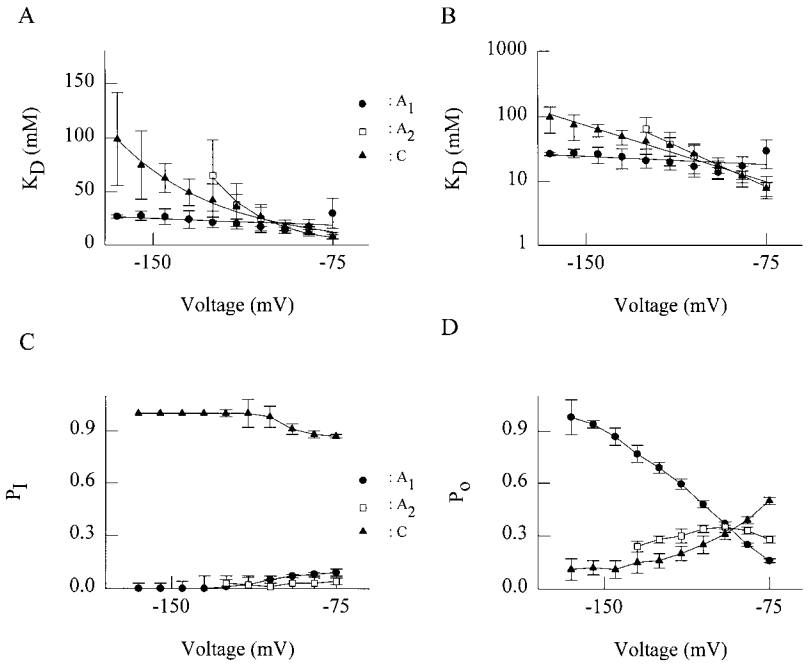

FIGURE 6. Voltage dependence of I^- binding in hClC-1. Voltage dependence of the apparent dissociation constants (K_D) for the three different kinetic states shown as linear (*A*) and semi-log (*B*) plots. Lines indicate fits of the Woodhull formula: $K_D = K_D(0\text{ mV})\ e^{-F\delta V/RT}$, where $K_D(0$ mV) denotes the estimated value at a membrane potential of 0 mV, and δ is the electrical distance measured from the extracellular side of the membrane. (*C*) Voltage dependence of the limiting values for the derived fractional current amplitudes at very high extracellular I^- concentration (p_I). (*D*) Voltage dependence of the limiting values for the derived fractional current amplitudes at zero extracellular [I^-] (p_o).

TABLE I

Parameters for I^- Binding to the External Binding Site

Kinetic state	K_D (0 mV)	δ*
	mM	
A_1	13.7±4.4	0.1±0.04
A_2	0.1±0.1	1.14±0.07
C	2.2±0.03	0.59±0.03

*Values for δ are given as the distance from the extracellular side of the membrane.

activating component (A_2) are more scattered than for the other two components. This suggests that this model is a reasonable first approximation of the interaction between I^- and hClC-1.

This analysis gives us the dissociation constant, K_D, for external I^- binding to the channel in each kinetic state (Fig. 6, *A* and *B*). For the fast deactivating component (A_1), K_D is nearly voltage independent. By contrast, for both the slow deactivating component (A_2) and the nondeactivating component, the K_D is voltage dependent and can be well fit with the Woodhull formula (Woodhull, 1973), giving the K_D (0 mV) and the electrical distance δ (Fig. 6, *A* and *B*, Table I). Furthermore, fits of the data in Fig. 5 with Eq. 2 provide limiting values of *P* at very high (p_1) (Fig. 6 *C*), or zero (p_o) (Fig. 6 *D*) I^- concentration that can be used to describe the fractional current amplitudes when all external binding sites are either occupied or unoccupied by I^-. The plot of the calculated p_o for the three different kinetic states resembles the experimentally determined voltage-dependent behavior of the fractional current amplitudes measured in the absence of I^- (Fahlke et al., 1996). By contrast, the plot of calculated p_1 for the three different states indicates that binding of external I^- locks the channel in the nondeactivating state (Fig. 6 *C*).

Block of hClC-1 by Internal I^-

To examine the effect of internal I^- on hClC-1, we initially recorded currents from inside-out patches excised from cells stably expressing the channel. Currents were recorded from the same patch before and after application of 50 mM NaI to the cytoplasmic face of the membrane. In the presence of 50 mM I^-, the inward current amplitude is greatly reduced, whereas the outward current is unchanged (Fig. 7, *A* and *B*). In addition to reduction of the inward current amplitude, there is an apparent slowing of the deactivation process (Fig. 7 *B*), and the pronounced inward rectification of the instantaneous current–voltage relationship is abolished (Fig. 7 *C*).

We next examined the concentration dependence of the effects of internal I^- on hClC-1 by using whole cell recording (Fig. 8). Currents recorded from cells exposed to various intracellular I^- concentrations were normalized to levels measured at the most positive test potential, a valid procedure in view of the demonstrated lack of effect of internal I^- on outward current. Fig. 8, *A* and *B* illustrates the concentration-dependent reduction of normalized inward current amplitude by internal I^-. The effects are consistent with intracellular I^- block of hClC-1 currents.

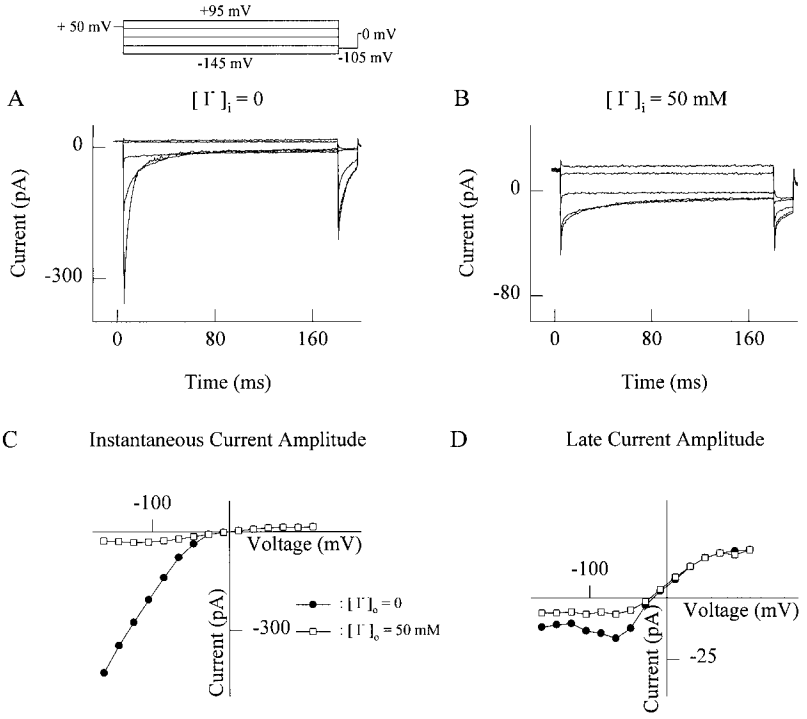

FIGURE 7. Effect of intracellular I^- on hClC-1 currents in excised inside-out patches from HEK-293 cells. The patch pipette was filled with standard extracellular solution, and the bath contained standard intracellular solution. The intracellular side of the patch was exposed to a solution containing (mM): 50 NaCl, 80 Na-gluconate, 2 $MgCl_2$, 5 EGTA, 10 HEPES, pH 7.4 (*A*); or (mM): 50 NaCl, 50 NaI, 30 Na-gluconate, 2 $MgCl_2$, 5 EGTA, 10 HEPES, pH 7.4 (*B*). (*A* and *B*) Current responses to voltage steps between −145 and +95 mV in 60-mV steps. Each voltage step was preceded by a 300-ms prepulse to +50 mV, and followed by a fixed test pulse to −125 mV. (*C* and *D*) Voltage dependence of the instantaneous and late current amplitudes as indicated.

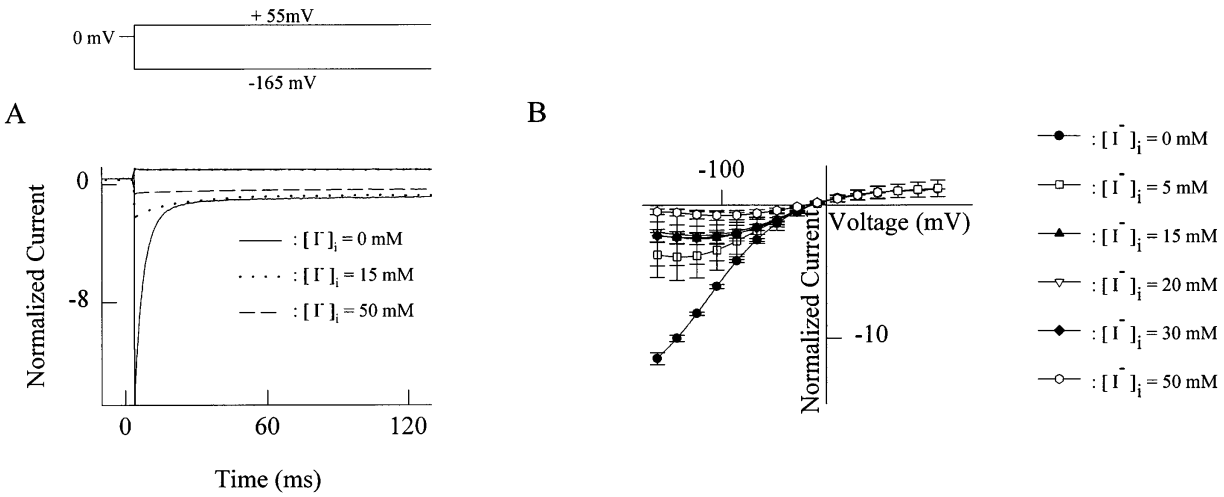

FIGURE 8. Effect of intracellular I^- on hClC-1 current in HEK-293 cells. (*A*) Current responses to voltage steps to −165 and +55 mV from a holding potential of 0 mV. Data shown are from three different cells exposed to three different internal I^- concentrations as indicated in the figure. Currents were normalized to the current amplitude measured at +55 mV. (*B*) Voltage dependence of the instantaneous current amplitude for different intracellular I^- concentrations. Iodide concentration was changed by replacing different amounts of Na-gluconate with NaI in a pipette solution containing (mM): 50 NaCl, 80 Na-gluconate, 2 $MgCl_2$, 5 EGTA, 10 HEPES, pH 7.4. Each point represents mean ± SEM from four cells. Current amplitudes were normalized to the value measured at +75 mV.

Block of hClC-1 by Other Internal Anions

Other anions exert similar effects on hClC-1 when present inside the cell. Fig. 9 *A* shows whole-cell recordings made from cells dialyzed intracellularly with 50 mM NaI (Fig. 9, *A* and *B*), 50 mM NaSCN (Fig. 9, *C* and *D*), or 50 mM $NaNO_3$ (Fig. 9, *E* and *F*). Compared with recordings made with standard pipette solutions, the deactivation process is much slower for all tested anions, but this kinetic effect is most pronounced for I^-. Analysis of the voltage dependence of the instantaneous current amplitude (Fig. 9, *B*, *D*, and *F*) shows that the degree of inward rectification of the instantaneous current amplitude is also decreased. These results indicate that several anions are able to interact with an internal ion binding site. As observed for the external binding site, the blocking potency of internally applied anions is correlated with the potency to change current kinetics (Fig. 9 *G*).

Kinetic Effects of Internal I^-

We further evaluated the kinetic changes caused by internal I^- by examining the channel with whole cell recording in the presence of various concentrations of NaI in the pipette solution. The time course of current deactivation measured under these conditions could be well fit with a function consisting of two exponentials and a constant term as described in METHODS. Both fast and slow deactivation time constants are increased in a concentration-dependent manner by intracellular I^-, and by contrast to the effect of external I^-, both deactivation time constants become voltage dependent (Fig. 10, *A* and *B*). Interestingly, however, the two time constants behave in opposite directions in response to voltage. Whereas the fast time constant increases with more negative test potentials (Fig. 10 *A*), the slow time constant decreases with hyperpolarization (Fig. 10 *B*).

We have previously modeled hClC-1 deactivation as a first order process mediated by a cytoplasmic gate (Fahlke et al., 1996). The occurrence of fast deactivating, slow deactivating, and constant current components corresponds with the existence of three populations of channels differing in the affinity of the internal vestibule of the ionic pore for this blocking particle. For each kinetic state in the presence of internal I^-, there will be a mixed population of channels whose internal binding site will be occupied or not occupied by I^- (see Scheme 2). Therefore, both deactivation time constants in the presence of internal I^- will be a weighted mixture resulting from these two channel populations. By analogy to Eq. 2, we can relate the I^- dissociation constant (K_D) for the internal binding site to the deactivation time constants by the following formula:

$$\tau_i^{-1} = \tau_{max}^{-1} + \frac{[I^-]}{[I^-] + K_D}(\tau_{min}^{-1} - \tau_{max}^{-1}) \quad (4)$$

where τ_i is either the fast (τ_1) or slow (τ_2) deactivation time constant determined in the presence of internal I^-, and τ_{min}, τ_{max}, and K_D are fit parameters. We restricted this analysis to the fast- and slow-deactivating components because, in the presence of internal I^-, we are unable to distinguish the constant component from an incomplete deactivation in the fast or slow mode. We assumed that intracellular Cl^- equilibrates with the internal binding site much faster than the deactivation

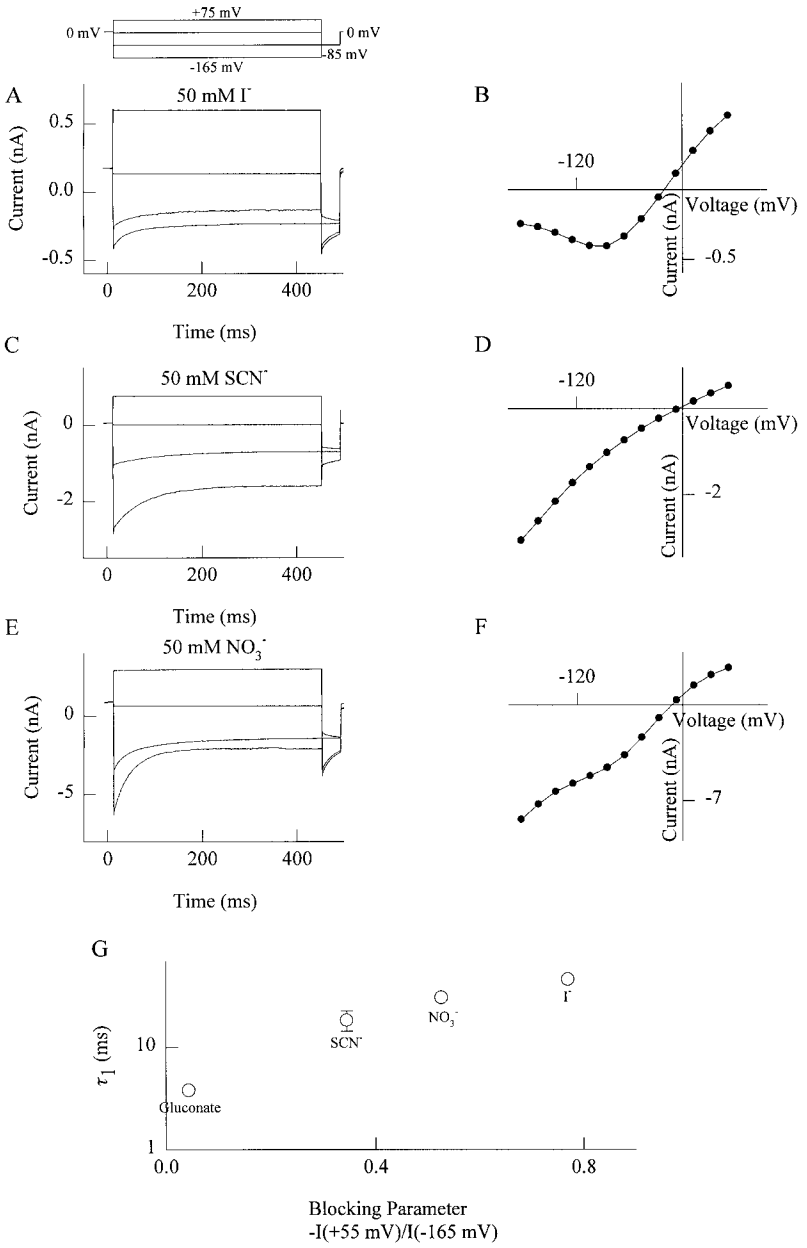

FIGURE 9. Effect of different intracellular anions on hClC-1 stably expressed in HEK-293 cells. (*A, C,* and *E*) Current responses to voltage steps from a holding potential of 0 mV to test potentials between −165 and +75 mV in 80-mV steps. Each step is followed by a test potential of −85 mV. Cells were bathed in standard extracellular solution and perfused intracellularly with a solution containing (mM): 50 NaCl, 50 NaX, 30 Na-gluconate, 2 $MgCl_2$, 5 EGTA, 10 HEPES where X denotes I^- (*A*), NO_3^- (*C*), or SCN^- (*E*). (*B, D,* and *F*) Voltage dependence of the instantaneous current amplitudes from recordings shown in *A, C,* and *E*. (*G*) Correlation of the potency to block Cl^- currents from the intracellular site and the fast deactivation time constant τ_1 measured at a test potential of −145 mV. We defined a blocking parameter by dividing the current amplitude measured at +55 mV (which is not affected by intracellular anions) by the amplitude at −145 mV for each cell. Data points represent mean ± SEM from three cells.

process. We determined K_D values for these two kinetic states at different test potentials (Fig. 11, *A* and *B*). The two kinetic states analyzed in this manner exhibit differences in their affinities for I^- and in the voltage dependence of the effect (Fig. 11 *C*, Table II). Whereas the fast deactivating state is characterized by a voltage-dependent K_D, the values for the slow deactivating component are nearly voltage independent. As expected, the derived values for τ_{min} (Fig. 11 *D*) closely resemble the experimentally determined values measured in the absence of internal I^- (see Fig. 10). For both the fast and slow processes, the fit parameter τ_{max}^{-1} is zero, indicating that a channel internally occupied by I^- cannot close.

Multiple Occupancy of the hClC-1 Conduction Pathway

The experiments described above clearly demonstrate the distinct effects of external versus internal I^- on hClC-1, and suggest the presence of two separate ion binding sites within the ion conduction pathway of hClC-1. The binding site accessible to internal I^- appears to interact more directly with the channel closing mechanism, whereas the externally accessible site has effects on the voltage-dependent distribution of channels in the aforementioned three kinetic states. In our previously described gating model of hClC-1, the latter observation would fit with an alteration in voltage sensing caused by external I^- (Fahlke et al., 1996).

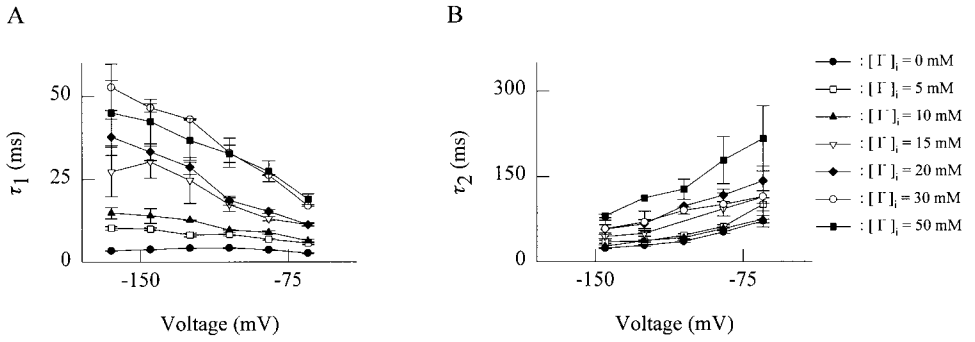

FIGURE 10. Effect of intracellular I^- on deactivation time constants. (*A*) Voltage dependence of the fast deactivation time constants (τ_1) for different intracellular I^- concentrations. Each point represents mean ± SEM from four cells. (*B*) Voltage dependence of the slow deactivation time constants (τ_2) for different intracellular I^- concentrations.

The evidence suggesting that hClC-1 has two distinct ion binding sites within its conduction pathway raises the question of whether these sites can be occupied simultaneously. One approach to address whether hClC-1 has a multi-ion pore is by testing for concentration dependence of the permeability ratio under biionic conditions (Hille, 1992). Therefore, we measured current reversal potentials with whole-cell patch clamp in HEK-293 cells stably expressing hClC-1 under conditions in which Cl^- was the only extracellular permeant anion and I^- was the only intracellular permeant anion. Measurements made with various concentrations of Cl^- and I^- in a fixed ratio revealed concentration dependence of the reversal potential and, by inference, of the P_I/P_{Cl} permeability ratio (Fig. 12 *A*). This finding is consistent with ion–ion interactions within a multi-ion pore.

A second line of evidence supporting the idea that hClC-1 is a multiply occupied pore comes from the electrical distance as obtained from Woodhull fits to the voltage dependence of the I^- dissociation constant to the slow deactivating component (Table I). This number is greater than one, a finding typical for multi-ion channels (Hille and Schwarz, 1978).

Based on results demonstrated for ClC-0 (Pusch et al., 1995), we also tested for anomalous mole fraction behavior in hClC-1 expressed in oocytes using mixtures of Cl^- with either I^- or SCN^-. Fig. 12, *B* and *C* shows plots of normalized peak instantaneous current versus the mole fraction of the tested anion. In these experiments, we observed no minimum value for normalized current at any tested mole fraction. We also tested mixtures of Cl^- with NO_3^- and similarly did not observe a minimum value in current versus mole fraction plots.

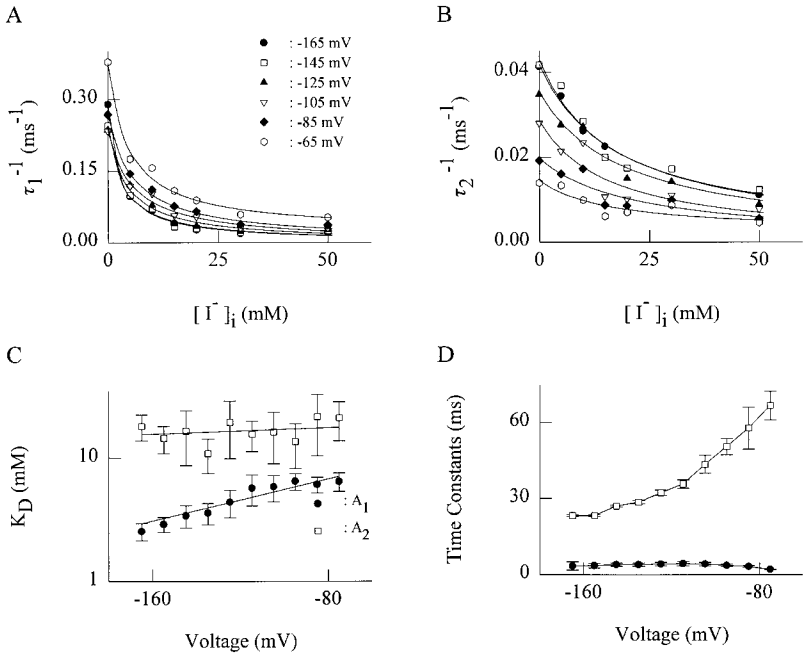

FIGURE 11. Intracellular I^- concentration dependence of hClC-1 deactivation. Reciprocal deactivation time constants determined at six different test potentials in the presence of different intracellular I^- concentrations. (*A*) I^- concentration dependence of the fast deactivation time constant (τ_1). (*B*) I^- concentration dependence of the slow deactivation time constant (τ_2). In *A* and *B*, solid lines represent fitted hyperbola to the measured data (see text), and each point represents mean ± SEM for at least three cells. (*C*) Voltage dependence of K_D determined from data fits shown in *A* and *B*. (●) Fast deactivating state, (□) slow deactivating state. Lines indicate Woodhull fits: $K_D = K_D(0\text{ mV})\, e^{F\delta V/RT}$, where $K_D(0\text{ mV})$ denotes the estimated value at a membrane potential of 0 mV and δ the electrical distance measured from the extracellular side of the membrane. (*D*) Voltage dependence of τ_{min} for the derived values for fast (τ_1, ●) and slow (τ_2, □) deactivation time constants.

TABLE II

Parameters for I^- Binding to the Internal Binding Site

Kinetic state	K_D (0 mV)	δ*
	mM	
A_1	14.8±2.2	0.75±0.04
A_2	19.9±7.2	0.95±0.07

*Values for δ are given as the distance from the extracellular side of the membrane.

The absence of anomalous mole fraction behavior in hClC-1 does not exclude a multi-ion permeation mechanism (Hille, 1992).

DISCUSSION

Functional Alterations of Ion Binding Sites by Voltage-dependent Gating

In this paper, we extend our earlier observations suggesting the existence of two distinct ion binding sites in the hClC-1 conduction pathway (Fahlke et al., 1997*a*). Specifically, we have characterized in more detail the ability of I^- and other anions to block hClC-1 when applied from both sides of the cell membrane. Examining the effects of external versus internal anion block of hClC-1 has helped us distinguish two fundamentally different ion-channel interactions by virtue of their distinct effects on the kinetics and voltage dependence of channel gating. The ion binding sites responsible for mediating block of Cl^- current appear to be identical to those through which anions exert their effects on gating based upon the close correlation of the two phenomena (Figs. 3 and 9).

Interactions between blocking anions and the channel pore depend upon the kinetic state, as illustrated by the effect of voltage-dependent gating events on the quantitative parameters of external and internal ion binding (Tables I and II). By examining the I^- concentration dependence of two parameters, fractional current amplitudes (reflecting external I^- effects) and the deactivation time constants (reflecting internal I^- effects), we were able to discern remarkable changes in the apparent affinity of hClC-1 for I^- during voltage-dependent gating transitions. In addition, we observed significant alterations in the electrical distance of I^- binding occurring with changes in the kinetic state. These state-dependent changes in ion binding reveal transitional alterations in the interactions between the open pore and blocking anions as a particular mechanistic feature of voltage-dependent gating in hClC-1. These observations suggest that voltage-dependent gating events may be accompanied by structural rearrangements within the pore that alter the location of the ion binding sites within the electrical field and affect ion binding affinity. These data support our previously published hypothesis of voltage-dependent transitions occurring between conducting states in hClC-1 (Fahlke et al., 1996).

The observed differences in the electrical distances of the binding sites are quite large, and seem to indicate drastic structural rearrangements of the pore during gating. However, electrical distances are not comparable with physical distances because of the inadequacy of the constant field assumption. In multiply

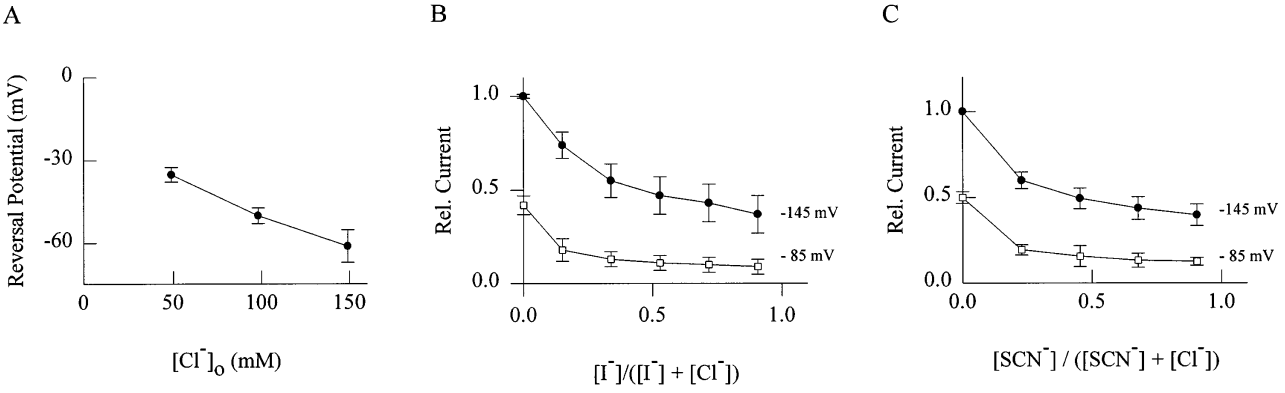

FIGURE 12. Concentration dependence of the reversal potential and mole fraction behavior in hClC-1. (*A*) Dependence of the reversal potential on extracellular Cl^- concentration measured in HEK-293 cells. Current reversal potentials were measured under biionic conditions with I^- as the only permeant intracellular and Cl^- as the only permeant extracellular anion. Iodide and Cl^- concentrations were changed proportionally. (*B* and *C*) Mole fraction behavior of hClC-1 instantaneous current amplitudes measured in *Xenopus* oocytes at −145 and −85 mV for mixtures of Cl^- and I^- (*B*), and Cl^- and SCN^- (*C*). Instantaneous current amplitudes were measured on three different cells For each oocyte, five different mole fractions were tested. The mole fraction was changed by replacing equimolar amounts of NaCl with either NaI or NaSCN. Relative current was calculated by normalizing instantaneous current amplitudes to the value obtained at −145 mV measured in ND-96 solution.

occupied ion channels (Hille and Schwarz, 1978), measured electrical distances can be much greater than the physical distances and may even exceed unity. In these ion channels, even slight physical movements of ion binding sights can cause large differences in the measured electrical distances.

Relationship between Ion Permeation and Gating in hClC-1

It is very apparent from this study of hClC-1 and previously published work on the *Torpedo* channel, ClC-0 (Pusch et al., 1995; Chen and Miller, 1996), that ion permeation and gating are functionally linked in ClC channels. At the present time, there are differing opinions regarding the explanation for this functional linkage. In ClC-0, evidence has been presented that translocation of the permeating ion through the conduction pathway confers the majority of the voltage dependence of activation, and that there is little or no contribution of intrinsic protein charge movement to this process (Chen and Miller, 1996).

We have presented a different viewpoint on the mechanism of voltage-dependent gating in hClC-1 (Fahlke et al., 1995, 1996). Based upon macroscopic analysis of gating, we have proposed a model in which voltage-dependent conformational changes modulate gating by altering the affinity of the channel for a cytoplasmic blocking particle. These voltage-dependent conformational changes result in three different kinetic states in hClC-1 distinguished by their time course of deactivation. This voltage-responsive phenomenon can be modulated by permeant ions. As presented in this paper, occupation of the external binding site by I^- locks the channel in the nondeactivating state.

Chen and Miller (1996) recently examined the Cl^- dependence of ClC-0 activation using measurements of opening rate constants derived from single channel recording of purified channels reconstituted into planar lipid bilayers. They found that the external Cl^- concentration giving a half-maximal opening rate was not affected by the membrane potential, and this observation led them to conclude that initial binding of Cl^- to the closed channel is voltage independent. Unlike the closed channel, open ClC-0 channels in lipid bilayers exhibit two ion binding sites that can sense the membrane potential and are located at electrical distances of 0.35 and 0.65 from the *cis* side (White and Miller, 1981). Although it is not entirely clear, it seems logical that the ion binding site in the closed channel that mediates Cl^- activation is the same as the site accessible from the external solution in the open channel. In hClC-1, it is interesting to note that the site accessible to the external solution is minimally sensitive to voltage when the channel exists in the fast deactivating mode ($\delta = 0.1$; Table I), but the same site is located more deeply in the electric field in both the slow deactivating and constant current conformations.

Mechanism of Ion Selectivity of hClC-1 Channels

The observation that almost every tested anion is permeant and yet capable of blocking the channel from both sides of the membrane provides information about the mechanism of ion selectivity in hClC-1. The qualitative similarities of effects of the various tested anions on current kinetics suggests that all of the anions we tested interact with the same binding sites. This idea is reinforced by the observed correlation between the potency to block inward current with the ability to alter macroscopic gating properties (Figs. 3 and 9). The two sites differ slightly in ionic rank order blocking potency (external site: $SCN > I > NO_3 > CH_3SO_3 > Br$; internal site: $I > NO_3 > SCN$). By conventional wisdom, anions that block Cl^- current do so because of higher affinity for a binding site within the conduction pathway. For hClC-1, the permeability sequence determined by examining reversal potentials in the presence of different external anion composition ($Cl > SCN > Br > NO_3 > I > CH_3SO_3$) (Fahlke et al., 1997*a*) correlates inversely with the blocking potency sequence of the internal site, but less well with that of the external site. In qualitative terms, all of the tested anions less permeant than Cl^- exert a blocking action. This is consistent with a mechanism of ion selectivity in hClC-1 based on differential ion binding rather than repulsion or size exclusion.

Binding of ions to sites within the conduction pathway requires replacement of ion–solvent with ion–channel interactions (Eisenman and Horn, 1983; Hille, 1992), a process in which hydration energy is spent and electrostatic energy is released. The binding of larger (i.e., I^-) or polyatomic (i.e., SCN^-, NO_3^-, $CH_3SO_3^-$) anions more tightly than Cl^- to the hClC-1 binding sites suggests that hydration forces dominate the ion–channel interaction consistent with weak binding sites in Eisenman terminology (Wright and Diamond, 1977; Eisenman and Horn, 1983). These ion binding sites could conceivably consist of either a fixed charge with a large radius, or a weak dipole (Wright and Diamond, 1977).

The measurement of permeability for different-sized anions can provide information about the hClC-1 pore size. Among the larger anions tested, CH_3SO_3 (ionic diameter $\cong$ 0.50 nm; see Halm and Frizzell, 1992) can traverse the pore, whereas gluconate (ionic diameter = 0.59 nm) is impermeant, thus giving an estimate of the minimum pore diameter between 0.5 and 0.6 nm. The inability of gluconate to permeate or block the hClC-1 pore suggests that both ion binding sites are located in a narrow part of the conduction pathway. This is in clear contrast to voltage-gated sodium and potassium channels in which a variety of blockers can bind to a

wide vestibule but are impermeant because of size exclusion (Hille, 1992).

The minimum diameter of the hClC-1 pore appears to be considerably larger than those found in the conduction pathway of voltage-gated potassium channels, but smaller than that of the nicotinic acetylcholine receptor. This estimated minimum pore diameter for hClC-1 is similar to apical membrane Cl^- channels of secretory epithelial cells (Halm and Frizzell, 1992) and to the skeletal muscle calcium channel (McCleskey and Almers, 1985).

Conclusion

In summary, the experimental data we present here provides new insights into the nature of the ion conduction pathway in hClC-1. Our studies suggest that hClC-1 has a rather wide ionic pore that is multiply occupied, and is functionally characterized by two distinct ion binding sites. Both sites appear to be weak interacting sites in Eisenman terminology, and the mechanism of ion selectivity in hClC-1 involves differential ion binding. Lastly, we provide evidence that the hClC-1 pore is dynamic in that conformational changes within the conduction pathway underlie the functional link between gating and permeation. These results provide a framework for understanding ion permeation in hClC-1 and will facilitate future experiments aimed at defining the structure and function of ClC channels.

We are grateful to Dr. Louis DeFelice and Dr. Richard Horn for their critical reviews of the manuscript.

This work was supported by grants from the Muscular Dystrophy Association (A.L. George, Jr. and Ch. Fahlke) and the Lucille P. Markey Charitable Trust (A.L. George, Jr.). C. Dürr was on leave of absence from Kreiskrankenhaus Krumbach (Krumbach, Germany). Ch. Fahlke was supported by the Deutsche Forschungsgemeinschaft (DFG, Fa301/1-1), and A.L. George, Jr. is a Lucille P. Markey Scholar.

Original version received 7 February 1997 and accepted version received 26 August 1997.

REFERENCES

Beck, C.L., Ch. Fahlke, and A.L. George, Jr. 1996. Molecular basis for decreased muscle chloride conductance in the myotonic goat. *Proc. Natl. Acad. Sci. USA.* 93:11248–11252.

Chen, T.Y., and C. Miller. 1996. Nonequilibrium gating and voltage dependence of the ClC-0 Cl^- channel. *J. Gen. Physiol.* 108:237–250.

Dascal, N., T.P. Snutch, H. Lübbert, N. Davidson, and H.A. Lester. 1986. Expression and modulation of voltage-gated calcium channels after RNA injection in *Xenopus* oocytes. *Science (Wash. DC).* 231:1147–1150.

Eisenman, G., and R. Horn. 1983. Ionic selectivity revisited: the role of kinetic and equilibrium processes in ion permeation through channels. *J. Membr. Biol.* 76:197–225.

Fahlke, Ch., R. Rüdel, N. Mitrovic, M. Zhou, and A.L. George, Jr. 1995. An aspartic acid residue important for voltage-dependent gating of human muscle chloride channels. *Neuron.* 15:463–472.

Fahlke, Ch., A. Rosenbohm, N. Mitrovic, A.L. George, Jr., and R. Rüdel. 1996. Mechanism of voltage-dependent gating in skeletal muscle chloride channels. *Biophys. J.* 71:695–706.

Fahlke, Ch., C.L. Beck, and A.L. George, Jr. 1997*a*. A mutation in autosomal dominant myotonia congenita affects pore properties of the muscle chloride channel. *Proc. Natl. Acad. Sci. USA.* 94: 2729–2734.

Fahlke, Ch., T.J. Knittle, C.A. Gurnett, K.P. Campbell, and A.L. George, Jr. 1997*b*. Subunit stoichiometry of human muscle chloride channels. *J. Gen. Physiol.* 109:93–104.

Fahlke, Ch., and R. Rüdel. 1995. Chloride currents across the membrane of mammalian skeletal muscle fibres. *J. Physiol. (Camb.).* 484:355–368.

George, A.L., M.A. Crackower, J.A. Abdalla, A.J. Hudson, and G.C. Ebers. 1993. Molecular basis of Thomsen's disease (autosomal dominant myotonia congenita). *Nat. Genet.* 3:305–310.

Halm, D.R., and R.A. Frizzell. 1992. Anion permeation in an apical membrane chloride channel of a secretory epithelial cell. *J. Gen. Physiol.* 99:339–366.

Hamill, O.P., A. Marty, E. Neher, B. Sakmann, and F.J. Sigworth. 1981. Improved patch-clamp techniques for high-resolution current recording from cells and cell-free membrane patches. *Pflügers Arch.* 391:85–100.

Hille, B. 1992. Ionic Channels of Excitable Membranes. 2nd ed. Sinauer Associates Inc., Sunderland, MA. 607 pp.

Hille, B., and W. Schwarz. 1978. Potassium channels as multi-ion single-file pores. *J. Gen. Physiol.* 72:409–422.

Jentsch, T.J., K. Steinmeyer, and G. Schwarz. 1990. Primary structure of *Torpedo marmorata* chloride channel isolated by expression cloning in *Xenopus* oocytes. *Nature (Lond.).* 348:510–514.

Jentsch, T.J. 1994. Molecular biology of voltage-gated chloride channels. *Curr. Top. Membr.* 42:35–57.

Koch, M.C., K. Steinmeyer, C. Lorenz, K. Ricker, F. Wolf, M. Otto, B. Zoll, F. Lehmann-Horn, K.H. Grzeschik, and T.J. Jentsch. 1992. The skeletal muscle chloride channel in dominant and recessive human myotonia. *Science (Wash. DC).* 257:797–800.

McCleskey, E.W., and W. Almers. 1985. The Ca channel in skeletal muscle is a large pore. *Proc. Natl. Acad. Sci. USA.* 82:7149–7153.

Pusch, M., U. Ludewig, A. Rehfeldt, and T.J. Jentsch. 1995. Gating of the voltage-dependent chloride channel ClC-0 by the permeant anion. *Nature (Lond.).* 373:527–530.

Steinmeyer, K., R. Klocke, C. Ortland, M. Gronemeier, H. Jockusch, S. Gründer, and T.J. Jentsch. 1991. Inactivation of muscle chloride channel by transposon insertion in myotonic mice. *Nature (Lond.).* 354:304–308.

Tokimasa, T., and R.A. North. 1996. Effects of barium, lanthanum, and gadolinium on endogenous chloride and potassium currents in *Xenopus* oocytes. *J. Physiol. (Camb.).* 496:677–686.

White, M.M., and C. Miller. 1981. Probes of the conduction process of a voltage-gated Cl^- channel from *Torpedo* electroplax. *J. Gen. Physiol.* 78:1–18.

Woodhull, A.M. 1973. Ionic blockage of sodium channels in nerve. *J. Gen. Physiol.* 61:687–708.

Wright, E.M., and J.M. Diamond. 1977. Anion selectivity in biological systems. *Physiol. Rev.* 57:109–156.